Available online at www.sciencedirect.com
SCIENCE DIRECT
Journal of Molecular Catalysis A: Chemical 244 (2006) 1–7
JOURNAL OF MOLECULAR CATALYSIS A: CHEMICAL
www.elsevier.com/locate/molcata

Synthesis, characterization and activity study of $SO_4^{2-}/Ce_xZr_{1-x}O_2$ solid superacid catalyst

Benjaram M. Reddy *, Pavani M. Sreekanth, Pandian Lakshmanan, Ataullah Khan

Inorganic and Physical Chemistry Division, Indian Institute of Chemical Technology, Uppal Road, Tarnaka, Hyderabad, AP 500007, India

Received 9 August 2005; received in revised form 31 August 2005; accepted 31 August 2005
Available online 3 October 2005

Abstract

Sulfated $Ce_xZr_{1-x}O_2$ catalyst was found to exhibit solid super-acidity and good catalytic activity for synthesis of β-amino ketones by a three-component Mannich type reaction in the liquid phase under solvent free conditions at ambient temperature. To make the sulfated $Ce_xZr_{1-x}O_2$ catalyst, Ce-Zr hydroxide gel was prepared by a coprecipitation method and SO_4^{2-} ions were deposited by treating the gel with sulfuric acid and calcined at 923 K. Surface and bulk properties of the $Ce_xZr_{1-x}O_2$ and $SO_4^{2-}/Ce_xZr_{1-x}O_2$ samples were investigated by means of X-ray powder diffraction, thermogravimetry, ammonia-TPD, Raman spectroscopy and BET surface area methods. Characterization results indicate that impregnated SO_4^{2-} ions strongly influence the physicochemical characteristics of the $Ce_xZr_{1-x}O_2$ solid solution. Powder XRD profiles reveal the presence of cubic $Ce_{0.5}Zr_{0.5}O_2$ in the case of unpromoted sample and tetragonal $Ce_{0.16}Zr_{0.84}O_2$ phase along with zirconium sulfate compounds in the case of SO_4^{2-} promoted sample. In particular, the XRD and Raman results suggest a selective interaction of the sulfate ions with zirconia portion of the $Ce_xZr_{1-x}O_2$ solid solution leading to the formation of zirconium sulfate compounds. The NH_3-TPD profiles indicate significant changes in the distribution of acid sites on the $Ce_xZr_{1-x}O_2$ upon sulfation. The $SO_4^{2-}/Ce_xZr_{1-x}O_2$ sample exhibits strong as well as super-acidic sites.

Keywords: Solid superacid; Sulfated zirconia; Ceria–zirconia; Sulfated ceria–zirconia; Mannich reaction; Ammonia-TPD

1. Introduction

The use of conventional acids such as H_2SO_4, HF, $AlCl_3$, BF_3, SbF_5, H_3PO_4 and HCl for organic reactions pose significant risks in handling, containment and disposal due to their toxic and corrosive nature. Owing to high reactivity, ease of handling, recovery, low waste generation and environmental friendliness, heterogeneous solid acid catalysts are emerging as very attractive alternatives to the conventional homogenous acidic reagents. Among various solid acid catalysts such as zeolites, clays and heteropolyacids, the sulfated metal oxides, based on zirconium oxide have emerged as powerful catalysts due to their super-acidity, high reactivity at low temperatures and reusability [1,2]. The ZrO_2 when modified with sulfate ions results in a highly acidic material that exhibits superior catalytic activity than that of 100% sulfuric acid in many catalytic reactions [2,3–5]. However, the unsupported SO_4^{2-}/ZrO_2 catalyst suffers from the disadvantage of relatively small specific surface area and thereby limited availability of the acid sites. The term 'superacid' was first proposed by Conant in 1923 to describe acid systems that are stronger than conventional mineral acids. Later, Gillespie defined the superacid as "an acid system stronger than that of 100% sulfuric acid, i.e., $Ho \leq -12$" [6].

Sulfated zirconia with a large specific surface area has always been sought. The activity, selectivity and stability of sulfated zirconia catalysts were also improved by the addition of noble metals and transition metal oxides such as Ni and Fe [7–9]. In some instances, it has been claimed that metal promoter is necessary in order to produce acid sites by for example, hydrogen spillover that generate Brønsted acid sites [10–12]. Approaches like making mesoporous zirconia systems [13], supporting sulfated zirconia into the pores of ordered mesostructured materials

* Corresponding author. Tel.: +91 40 27160123; fax: +91 40 27160921.
E-mail addresses: bmreddy@iict.res.in, mreddyb@yahoo.com (B.M. Reddy).

1381-1169/$ – see front matter © 2005 Elsevier B.V. All rights reserved.
doi:10.1016/j.molcata.2005.08.054

[14] and other [15,16] methodologies have been attempted to overcome the problems associated with unsupported catalysts. Although mesostructured sulfated-zirconia materials have been successfully synthesized, their catalytic activities for *n*-butane isomerization were still relatively low or similar to that of conventional sulfated zirconia catalysts [17,18]. The incorporation of SO_4^{2-}/ZrO_2 into the pores of mesostructured materials has successfully generated catalysts which show stronger acid strength than that of the parent materials. However, the success is very limited since SO_4^{2-}/ZrO_2 blocks some of the pores and the specific surface area of the materials is thus significantly reduced [19]. In some cases, mesoporous materials modified by sulfated zirconia showed lower acid strength than that of conventional SO_4^{2-}/ZrO_2 catalysts [20].

Other reliable techniques adopted in order to improve the catalytic performance of sulfated zirconia catalysts include forming mixed oxides of zirconia with other transitional and non-transitional metals and sulfating them. Some mixed oxides exhibited strong surface acidity (Brønsted or Lewis) due to the generation of excess negative or positive charge in the model structure of the binary oxides. For example, the SiO_2–ZrO_2 [21] and Al_2O_3–ZrO_2 [22] combinations lead to very strong acidic properties, whereas TiO_2–ZrO_2 was not only a strong acid, but also had a distinct basicity [23,24]. Recently, SnO_2 [25] and Ga_2O_3 [26] incorporated ZrO_2 and promoted with sulfate ions were also reported which show good acidic properties and an improved catalytic performance.

Among zirconia based mixed oxides, the CeO_2–ZrO_2 combination has emerged as a fascinating catalytic material and attracted much attention recently owing to their superior oxygen storage/release and redox properties [27]. The incorporation of zirconium cations into the ceria unit cell or vice versa modifies the surface acid–base sites, as the exposed Ce^{4+} and Zr^{4+} ions act as Lewis acid sites and O^{2-} ions as Brønsted or Lewis base sites. Both CeO_2 and ZrO_2 exhibit the same metal–oxygen stoichiometry but possess different ionic characters. Cerium oxide is considered to be more ionic than zirconium oxide. The acid strength of the mixed oxides varies depending on the charge to radius ratio of the cations as well. The Zr^{4+} ion has an ionic radius of 0.84 Å, which is smaller than that of Ce^{4+}(0.97 Å) and is expected to generate strong acid sites in their solid solutions [28]. Moreover, surface hydroxyl groups could be generated due to dissociative adsorption of water on highly polar M_1–O–M_2 bonds. In this direction, we were interested to investigate the effect of sulfation on the physicochemical characteristics of CeO_2–ZrO_2 solid solutions, and to explore their acidic properties. In the present study, the Ce–Zr solid solution hydroxide gel was synthesized by a homogenous co-precipitation method and impregnated with sulfate ions to obtain the novel $SO_4^{2-}/Ce_xZr_{1-x}O_2$ solid superacid catalyst. The prepared catalyst and its precursor were characterized by means of X-ray diffraction (XRD), thermal analysis (TGA/DTA), BET surface area, Raman spectroscopy (RS) and NH_3-temperature programmed desorption (TPD) techniques. The catalytic activity of the $SO_4^{2-}/Ce_xZr_{1-x}O_2$ sample was evaluated in the liquid phase for an interesting three-component Mannich type reaction at room temperature under solvent free conditions.

2. Experimental

2.1. Catalyst preparation

The $SO_4^{2-}/Ce_xZr_{1-x}O_2$ (SCZ) catalyst was prepared by adopting a two-step route. In the first stage Ce–Zr hydroxide gel was prepared and in the second stage sulfate ions were impregnated over its surface. The $Ce(OH)_4$–$Zr(OH)_4$ (1:1 mole ratio based on oxides) was obtained by precipitating a mixture solution of ammonium cerium nitrate $[(NH_4)_2Ce(NO_3)_6{\cdot}6H_2O]$ and zirconium nitrate $[Zr(NO_3)_4{\cdot}6H_2O]$ with dilute aqueous ammonia solution (pH 8) under vigorous stirring. Thus, obtained precipitate was filtered, washed and then dried at 373 K for 12 h. The uncalcined hydroxide gel was sulfated by adding a measured volume of 0.5 M H_2SO_4 solution, so as to reach the equivalence of 5 ml of pure H_2SO_4 per gram of $Ce(OH)_4$–$Zr(OH)_4$ gel. This process was performed under mechanical stirring (shaker) and maintained for 1 h, subsequently dried at 393 K for 3 h and calcined at 923 K for 4 h. The finished catalyst was activated at 523 K for 5 h in vacuum before catalytic runs. An unpromoted $Ce_xZr_{1-x}O_2$ (CZ) solid solution was also prepared for comparison purpose by calcination of the hydroxide gel at 923 K for 4 h.

2.2. Catalyst characterization

Powder X-ray diffraction (XRD) patterns were recorded on a Siemens D-5000 diffractometer, using Ni-filtered Cu Kα (0.15418 nm) radiation source. Crystalline phases were identified by comparison with the reference data from International Centre for Diffraction Data (ICDD) files. The BET surface areas were measured by N_2 adsorption at liquid N_2 temperature using a Micromeritics Gemini 2360 instrument. Raman spectra were obtained on a DILOR XY spectrometer equipped with a liquid nitrogen cooled CCD detector. The emission line at 514.5 nm from an Ar^+ ion laser (Spectra Physics) was focused on the sample under the microscope, and width of the analyzed spot was ~1 μm. The power of the incident beam on the sample was 3 mW. The wavenumber values reported from the spectra are accurate to within 2 cm^{-1}. The NH_3-temperature programmed desorption (TPD) measurements were carried out on an Autochem 2910 instrument (Micromeritics, USA), in the temperature range 373–873 K at 10 K min^{-1} ramp. A thermal conductivity detector was used for continuous monitoring of the desorbed ammonia and the areas under the peaks were integrated using GRAMS/32 software. Prior to TPD studies, the sample was pretreated at 473 K for 1 h in a flow of ultra pure He gas (40 ml min^{-1}). After pretreatment, the sample was saturated with 10% ultra pure anhydrous ammonia gas (balance He; 75 ml min^{-1}) at 353 K for 2 h and subsequently flushed with He (60 ml min^{-1}) at 373 K for 2 h to remove the physisorbed ammonia.

2.3. Activity studies

All chemicals used in this study were commercially available. All the reactions were carried out in the liquid phase batch

mode taking the mixture of reactants and the catalyst in a round bottom flask and stirred at room temperature under nitrogen atmosphere for appropriate times. Completion of the reaction was monitored by TLC. After completion of the reaction, catalyst was recovered by simple filtration, and reused. The products were recovered from the filtrate, concentrated on a rotatory evaporator and chromatographed on a silica gel column to afford pure products (isolated yields). NMR and mass spectroscopic techniques were used to analyze the products and compared with the authentic samples.

3. Results and discussion

The temperature stability of the samples prepared in this study was investigated by TGA/DTA method. The obtained thermograms of uncalcined CZ and SCZ samples are presented in Fig. 1. The thermogram of the Ce–Zr hydroxide gel exhibits one prominent (∼373 K) and two less prominent (∼473 and 573 K) weight loss peaks. The major peak in the low-temperature region is due to the loss of physisorbed water, while the other two minor peaks are due to dehydration of water from micropores and subsequent dehydroxylation of the sample, respectively. In the case of sulfated sample, loss in weight between ambient to 923 K is nominal. At high temperatures beyond 923 K, two major weight loss regimes are observed (903–1103 K), which can be attributed to decomposition of surface sulfate groups at higher temperatures. This observation indicates the presence of at least two types of surface sulfate species in the case of SCZ sample. It is a known fact in the literature that when zirconia is mixed with other oxides, which influence the thermal stability of the resulting, sulfated materials. Recently, Signoretto et al. [26] reported that incorporation of gallium oxide into zirconia increases the thermal stability of the impregnated surface

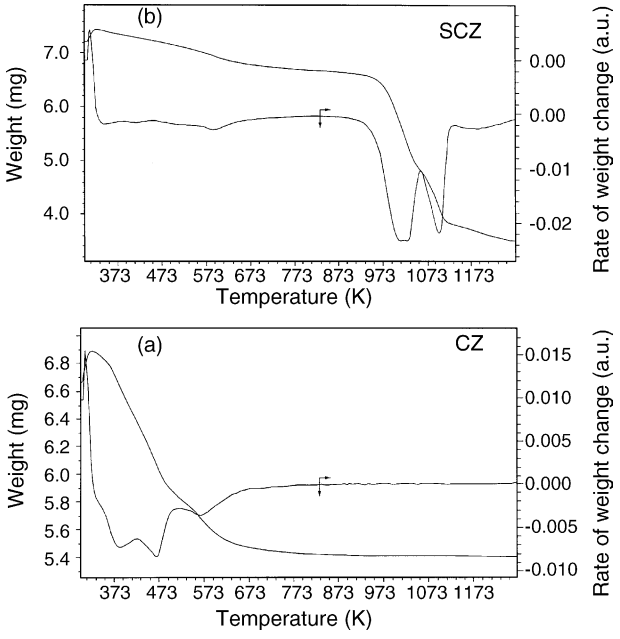

Fig. 1. TGA/DTA profiles of (a) $Ce(OH)_4$–$Zr(OH)_4$ and (b) SO_4^{2-}/$Ce(OH)_4$–$Zr(OH)_4$ samples before calcination.

Table 1
BET surface area, crystallite size and total acidity of $Ce_xZr_{1-x}O_2$ and $SO_4^{2-}/Ce_xZr_{1-x}O_2$ samples calcined at 923 K

Sample	Surface area ($m^2\ g^{-1}$)	Amount of ammonia desorbed (ml g^{-1})	Crystallite size (nm)
$Ce_xZr_{1-x}O_2$	84	1.35	4.5[a]
$SO_4^{2-}/Ce_xZr_{1-x}O_2$	126	19.98	n.d.[b]

[a] From XRD measurements.
[b] Not determined due to composition heterogeneity.

sulfate species when compared to that of ZrO_2 alone. Our earlier study also revealed similar type of weight loss peaks in the case of SO_4^{2-}/Al_2O_3–ZrO_2 samples indicating the decomposition of different surface sulfate species at higher temperatures when compared to that of SO_4^{2-}/ZrO_2 sample [22]. Thus, the thermogravimetry studies reveal that ceria enhances the thermal stability of the SO_4^{2-}/ZrO_2 catalyst.

The as synthesized $Ce(OH)_4$–$Zr(OH)_4$ hydroxide gel exhibited a high specific surface area of 162 $m^2\ g^{-1}$. However, upon calcination at 923 K a drastic decrease in the surface area (84 $m^2\ g^{-1}$) due to crystallization of the sample is observed. The sulfate ion impregnated sample calcined at 923 K exhibited a BET surface area of 126 $m^2\ g^{-1}$ (Table 1). This is in agreement with previous literature reports where impregnated sulfate ions were found to enhance the surface area of the ZrO_2 when compared to that of other promoters such as Cr-, Mo-, W-oxides [22,29,30]. The increase in the surface area of sulfated samples is due to the formation of porous surface sulfate compounds between the sulfate species and the supporting oxides [30].

The powder X-ray diffraction patterns of CZ and SCZ samples calcined at 923 K are shown in Fig. 2. The unpromoted CZ sample exhibits broad diffraction patterns due to small particle size (Table 1) and poor crystallinity. Nevertheless, diffraction patterns attributable to a $Ce_{0.5}Zr_{0.5}O_2$ (PDF-ICDD 38-1436) phase could be identified from the XRD analysis indicating the formation of solid solution between Ce- and Zr-oxides. As can be noted from Fig. 2 that the diffraction patterns of CZ and

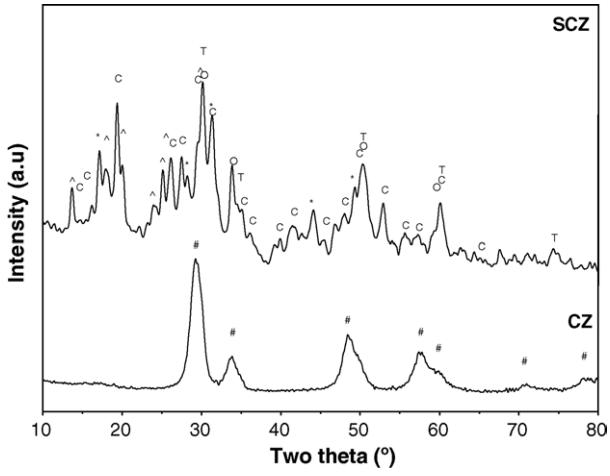

Fig. 2. XRD patterns of $Ce_xZr_{1-x}O_2$ (CZ) and $SO_4^{2-}/Ce_xZr_{1-x}O_2$ (SCZ) samples calcined at 923 K. Peak legends is as follows: (#) lines due to $Ce_{0.5}$ $Zr_{0.5}O_2$; (◯) lines due to $Ce_{0.16}Zr_{0.84}O_2$; (c) lines due to $Zr(OH)_2SO_4$; (∧) lines due to $Zr(SO_4)_2$; (T) lines due to *t*-ZrO_2; (*) lines due to *m*-ZrO_2.

SCZ samples differ very much indicating a strong influence of the impregnated sulfate ions. Close inspection of the XRD patterns pertaining to the SCZ sample reveal changes in the composition of the $Ce_xZr_{1-x}O_2$ phase and formation of zirconium sulfates. An interesting observation to be noted is that CZ sample exhibits diffraction patterns due to a cubic $Ce_{0.5}Zr_{0.5}O_2$ solid solution, while a tetragonal $Ce_{0.16}Zr_{0.84}O_2$ (PDF-ICDD 38-1437) phase could be identified in the case of SCZ sample. As per the literature, the presence of sulfate ions retards the crystallization process in the case of SO_4^{2-}/ZrO_2 samples and stabilize the tetragonal ZrO_2 modification [29]. Under identical calcination conditions, sulfated samples displayed a smaller crystallite size and increased amounts of tetragonal phase, in contrast to the corresponding non-sulfated samples [22]. This is primarily due to the influence of impregnated surface sulfate groups, which prevent the phase modification in the surface region from undergoing transformation [30,31]. It appears from the present study that sulfate ions exhibit similar influence on the ceria–zirconia mixed support. As can be noted from the diffractograms that the characteristic peaks corresponding to tetragonal zirconia ($2\theta = 30^\circ, 35^\circ$) are more intense than that of monoclinic zirconia phase ($2\theta = 28^\circ, 31^\circ$). The interaction of sulfate groups with mixed oxide supports leading to the formation of surface sulfates have been observed and change depending on the type of mixed oxide employed. In the case of sulfated titania–zirconia [32] formation of both $Ti_2(SO_4)_3$ and $Zr(SO_4)_2$ were noted. However, in the case of $SO_4^{2-}/Al_2O_3–ZrO_2$ sample only lines pertaining to the tetragonal zirconia phase were identified [22]. In the case of $SO_4^{2-}/CeO_2–ZrO_2$ sample lines due to a different type of surface zirconium sulfates namely zirconium sulfate hydroxide [$Zr(OH)_2SO_4$] (PDF-ICDD 26-1001) and zircosulfate [$Zr(SO_4)_2$] (PDF-ICDD 08-0495) could be manifested. No XRD lines pertaining to cerium sulfate compounds are observed. Similar findings were reported by Gao et al. [33], who prepared SO_4^{2-}/CeO_2 sample by macerating ceria nanoparticles in sulfuric acid solution and obtained CeO_2 particles with strongly bonded SO_4^{2-} groups on the surface. Their XRD patterns revealed characteristic peaks of ceria with no indication of cerium sulfate formation. It can be pointed out from the XRD patterns of the current SCZ sample that both tetragonal and monoclinic phases of zirconia are present and the former have gained more intensity.

Raman spectroscopy continues to be a powerful tool in catalysis in order to elucidate the structure of the active metal oxides supported on various catalytic support materials. To follow the changes in the structure due to sulfate modification, and to obtain additional structural information, Raman spectra of both samples were obtained. Fig. 3 represents the Raman spectra of the CZ and SCZ samples calcined at 923 K. The Raman spectrum of CZ sample exhibits typical bands due to $Ce_xZr_{1-x}O_2$ solid solution at 472, 630, 309, 267 cm^{-1}. Pure cerium dioxide exhibits strong band at 465 cm^{-1},which corresponds to the symmetric O–Ce–O stretching mode. This band appears at about 470 cm^{-1} for $CeO_2–ZrO_2$ (1:1 mole ratio) samples [34]. The Raman spectra of the CZ sample shows additional week bands at ~630, 309 and 267 cm^{-1}. The band observed at ~630 cm^{-1} corresponds to the non-degenerate Raman inactive LO mode of ceria [35].

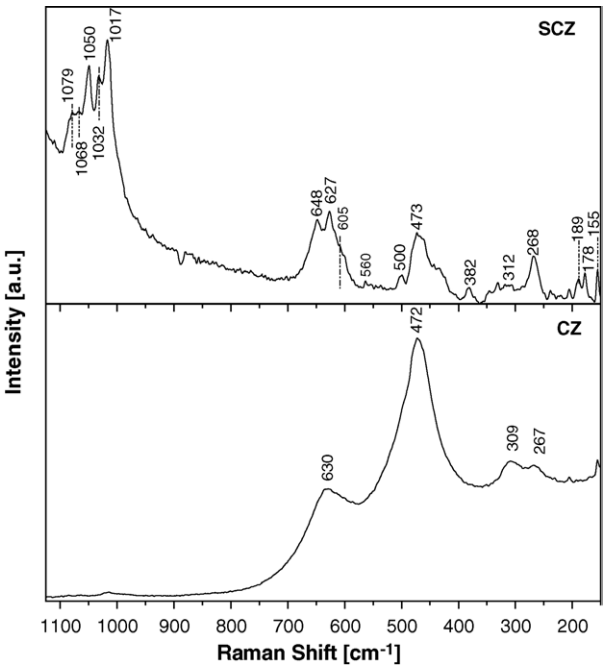

Fig. 3. Raman spectra of $Ce_xZr_{1-x}O_2$ (CZ) and $SO_4^{2-}/Ce_xZr_{1-x}O_2$ (SCZ) samples calcined at 923 K.

This band arises due to the perturbation of local M–O bond symmetry generated by oxygen vacancy. The appearance of week bands at 267 and 309 cm^{-1} could be attributed to the displacement of oxygen atoms from their ideal fluorite type lattice of cerium oxide [34,36]. Upon impregnating with sulfate ions, a drastic change in the Raman scattering pattern of the sample could be noted. As can be noted from Fig. 3 that the intensity of the RS band observed for CZ sample at 472 cm^{-1} decreased substantially in the case of sulfated sample. This indicates a significant change in the normal structure of the $CeO_2–ZrO_2$ solid solution. Furthermore, there is a gain in the intensity of the band at ~630 cm^{-1} upon sulfation which corresponds to an increase in the disorder in Ce–Zr–O bonding and oxygen vacancies, as discussed earlier. Noticeably, this is accompanied by the appearance of several other bands in the Raman spectrum of the SCZ sample. Interestingly, the zirconia features are not observed in the case of unpromoted CZ, but all zirconia related bands become obvious in the SCZ sample at the expense of cerium oxide features, indicating a very strong interaction of surface sulfate species with zirconia portion of the ceria–zirconia mixed oxide. The typical Raman bands due to tetragonal ZrO_2 are observed in the 150–700 cm^{-1} region. Strong bands at 268, ~460 and 648 cm^{-1} together with a shoulder at 605 cm^{-1} and smaller features around 312, 382 and 560 cm^{-1} are indicative for the tetragonal modification of zirconia. A sharp doublet observed at 178 and 189 cm^{-1} along with a sharp peak at 473 cm^{-1} are indicative for the presence of monoclinic zirconia [37]. The peaks pertaining to tetragonal and monoclinic modifications are in agreement with the XRD measurements. It is well known in the literature [37–40] that doping of zirconia with sulfate ions inhibits the formation of low-temperature monoclinic zirconia modification and leads to the stabilization of high-temperature

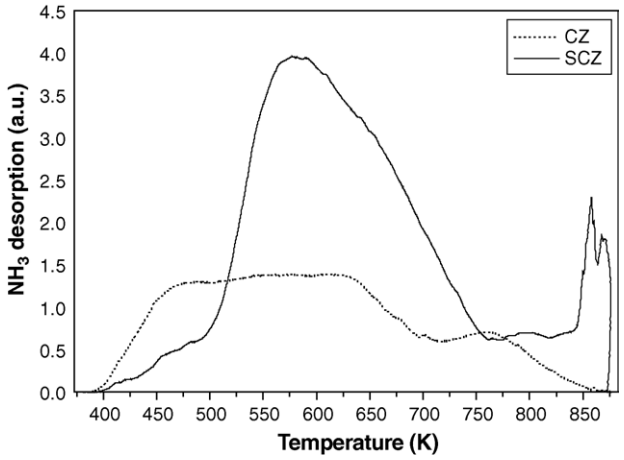

Fig. 4. Ammonia-TPD profiles of $Ce_xZr_{1-x}O_2$ (CZ) and $SO_4^{2-}/Ce_xZr_{1-x}O_2$ (SCZ) samples calcined at 923 K.

tetragonal phase. In the present study we observed the same phenomena in the case of sulfate ion promoted ceria–zirconia sample. The RS bands due to surface sulfates are visible in the range of 1000–1100 cm^{-1}(Fig. 3). The presence of bands in the Zr–O–S stretching region [41] at 1017, 1050 and 1032 cm^{-1} indicate the existence of more than one type of surface sulfate species, in line with XRD analysis [42], and support the formation of $[Zr(OH)_2SO_4]$ and $[Zr(SO_4)_2]$. The bands observed at 1068 and 1079 cm^{-1} could be tentatively assigned to stretching mode of surface sulfate groups connected to Ce. The substantial reduction in the intensity of the band at 472 cm^{-1} corresponding to the cubic fluorite type lattice of cerium oxide occurs upon sulfate modification and the zirconia related bands gain intensity showing a preferential interaction of the sulfate promoter with the zirconia portion leading to the formation of surface sulfates which have been revealed by the Raman spectroscopy study.

The TPD profiles of CZ and SCZ samples calcined at 923 K are shown in Fig. 4. Sulfate groups can generate strong acidity, when adsorbed on the mixed oxide supports. Sulfate species themselves are Lewis acids or by attracting electrons they generate Lewis acid centers on the oxide surfaces. These Lewis acid sites increase the Brønsted acid strength of the surface hydroxyl groups present on the surfaces. Further, the chemical states of the sulfate groups sometimes determine the acidity of the oxide surfaces. Calcination at higher temperatures leads to change in ionic to covalent character with S=O bond order close to 2, which is responsible for generating strong acidic active centers on the oxide surfaces. The profile of CZ sample reveals continuous NH_3 desorption in the 400–700 K temperature range, signifying a broad distribution of surface acid sites. The TPD profile of SCZ shows a different pattern signifying a marked increase in the acid strength and its distribution as there is a dramatic increase in the amount of desorbed ammonia (Table 1). This clearly indicates that impregnated sulfate groups strongly influence the acidic properties of ceria–zirconia mixed oxides. A broad ammonia desorption profile in the range 500–750 K with highest desorption around 580 K could be noted in the case of SCZ sample. This broad peak can be considered as an indication for the presence of high concentration of acid sites with moderate strength.

Table 2
SO_4^{2-}/Ce_x-$Zr_{1-x}O_2$ catalyzed three-component Mannich type reactions

Entry	Amine	Aldehyde	Ketone	Isolated yield (%)
1	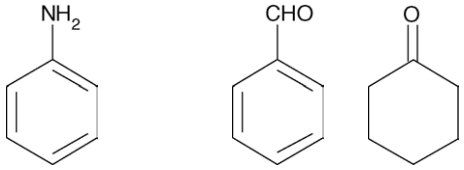			82
2	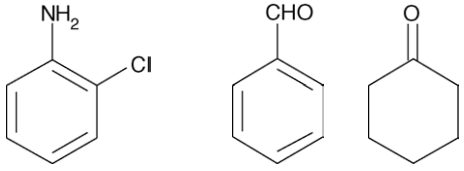			70
3	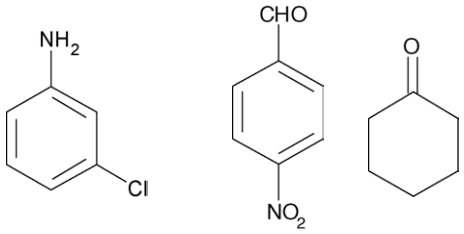			73
4	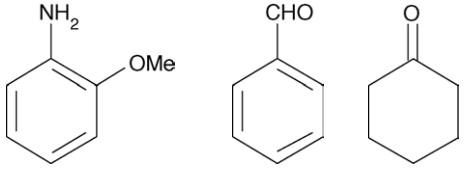			72
5	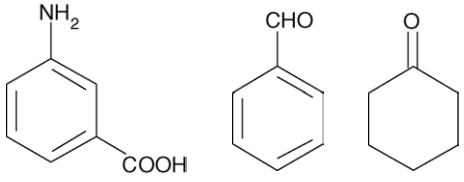			83
6	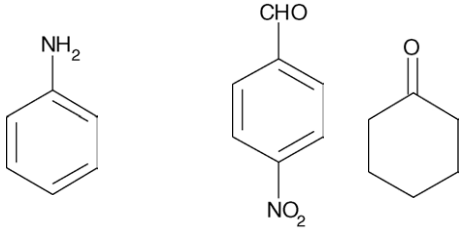			80

In addition to this broad peak, two high temperature desorption peaks are also observed at 857 and 870 K, respectively. The formation of superacid sites could be responsible for the observance of these high temperature desorption peaks in agreement with literature reports [43]. The position of ammonia desorption peak corresponding to the super-acidic sites is influenced by the nature of the mixed oxide with zirconia. In the case of sulfated alumina–zirconia and sulfated titania–zirconia samples a single high temperature desorption peak was observed at about 873 K [32,44]. However, in the case of sulfated ceria–zirconia sample

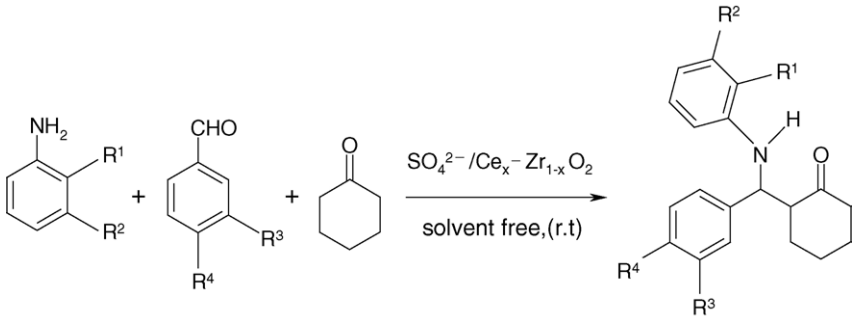

Scheme 1.

two close peaks at 857 and 870 K are noted. These observed high temperature peaks represent two different types of superacid sites with slightly differing their super-acidity.

The Mannich reaction is one of the most important methods in the preparation of β-amino carbonyl compounds and has wide applications in organic synthesis [45,46]. Mannich bases and derivatives such as, 1,3-amino alcohols, or Michael accepters, which are easily formed from Mannich bases are particularly versatile synthetic intermediates and find great use in, for example medicinal chemistry [47]. Several methods using a variety of Lewis acids in anhydrous conditions have been reported [48–52]. However, many of these methods involve toxic and hazardous Lewis acids including $TiCl_4$ in chlorinated solvents, which is not favorable from environmental point of view. Thus, in recent times a number of procedures using less hazardous Lewis and Brønsted acids in aqueous media have been developed [53–56]. In this study we successfully synthesized the β-amino carbonyl compounds by employing SO_4^{2-}/CeO_2-ZrO_2 catalyst (Scheme 1). In a typical reaction procedure benzaldehyde (0.53 g), aniline (0.47 g) and cyclohexanone (1.9 g) were taken in a 10 ml round bottomed flask (1:1:4 mole ratio of benzaldehyde, aniline and cyclohexanone), 0.1 g of $SO_4^{2-}/Ce_xZr_{1-x}O_2$ catalyst (20 wt.% with respect to the weight of benzaldehyde) was added to the reaction mixture. The reaction mixture was stirred in nitrogen atmosphere, under solvent free conditions and at room temperature. After the completion of the reaction (monitored by TLC), 10 ml of acetone was added to the reaction mixture and the catalyst was separated by filtration. The excess acetone was removed by using rotatory-evaporator and the product was purified by column chromatography. The wet catalyst was washed with dichloromethane many times, and recycled, to test the reusability of the catalyst. No appreciable change in the reactivity was observed for 2–3 runs. However, a progressive decrease in the activity was noticed with increasing number of cycles. The three-component Mannich-type reaction between benzaldehyde, aniline and cyclohexanone proceeded smoothly to afford 82% of product, with a *d*:*l* ratio of 82:18. Same reaction was carried out with dichloromethane as a solvent and 1:1:2 mole ratio of benzaldehyde, aniline and cyclohexanone, with 20% catalyst (with respect to weight of the benzaldehyde). There was no appreciable change in the yield of product compared to that of solvent free reaction. However, the reaction time increased when solvent was used for the reaction under identical conditions. The increase in the reaction temperature resulted in the lower yield of product, presumably due to the decreased stability of imines formed in the reaction. Hence, all the other examples were carried out under solvent free conditions and at 303 K. As can be noted from Table 2, in all reactions with various substituted aldehydes and amines, the corresponding Mannich bases were produced in good yields in short reaction times, in line with the observed strong acid sites of the sulfate promoted ceria-zirconia catalyst. The unpromoted CZ sample exhibited negligible activity under the identical reaction conditions, which clearly signifies the involvement of solid superacid sites in this reaction.

4. Conclusions

A novel solid super-acidic $SO_4^{2-}/Ce_xZr_{1-x}O_2$ catalyst was prepared from the uncalcined cerium-zirconium hydroxide gel obtained by a coprecipitation method and impregnating with sulfuric acid. The physicochemical characterization of the synthesized catalyst was carried out using various techniques including Raman spectroscopy and ammonia-TPD. The sulfate promoted ceria-zirconia catalyst exhibited good structural stability up to 913 K, above which thermal decomposition of surface sulfates occurs. The powder XRD and Raman spectroscopic results revealed a strong interaction of the sulfate ions with zirconia leading to the formation of surface sulfates, accompanied by the formation of a tetragonal $Ce_{0.16}Zr_{0.84}O_2$ phase. Sulfation of Ce–Zr hydroxide gel, and calcination at 923 K, resulted into significant changes in the physicochemical characteristics of CeO_2–ZrO_2 mixed oxide and its acidic character. The ammonia-TPD experiments showed that sulfation of ceria–zirconia mixed oxide can lead to the formation of super-acidic sites in the catalyst, while the unpromoted ceria–zirconia mixed oxide possesses only a broad distribution of week acid sites. The synthesized $SO_4^{2-}/Ce_xZr_{1-x}O_2$ catalyst was found to efficiently catalyze the three-component Mannich type reaction at room temperature. Mild reaction temperature under solvent free conditions, high yield of products and shorter reaction times are some of the advantages associated with these protocols.

Acknowledgment

P.M.S, A.K and P.L thank Council of Scientific and Industrial Research, New Delhi, for the award of senior research fellowships.

References

[1] K. Arata, Adv. Catal. 37 (1990) 165.
[2] K. Arata, Appl. Catal. A: Gen. 146 (1996) 3.
[3] A. Hino, K. Arata, J. Chem. Soc. Chem. Commun. 24 (1980) 1148.
[4] K. Tanabe, Mater. Chem. Phys. 13 (1995) 347.
[5] Y. Yamaguchi, Appl. Catal. 1 (1990) 61.
[6] R.J. Gillespie, T.E. Peel, J. Am. Chem. Soc. 95 (1973) 5173.
[7] C.Y. Hsu, C.R. Heimbuch, C.T. Armes, B.C. Gates, J. Chem. Soc. Chem. Commun. (1992) 1645.
[8] V. Adeeva, J.W. de Haan, J. Janchen, G.D. Lei, V. Schunemann, L.J.M. van de Yen, W.M.H. Sachtler, R.A. van Santen, J. Catal. 151 (1995) 364.
[9] E.J. Hollstein, J.T. Wei, C.Y. Hsu, US Patent 434,743,1989.
[10] K. Ebitani, J. Konishi, H. Hattori, J. Catal. 130 (1991) 257.
[11] K. Ebitani, J. Tsuji, H. Hattori, H. Kita, J. Catal. 135 (1992) 609.
[12] T. Shishido, H. Hattori, J. Catal. 161 (1996) 194.
[13] D.J. McIntosh, R.A. Kydd, Microporous Mesoporous Mater. 37 (2000) 281, and references therein.
[14] Y. Sun, L. Zhu, H. Lu, R. Wang, S. Lin, D. Jiang, F.S. Xiao, Appl. Catal. A: Gen. 237 (2002) 21.
[15] M.K. Mishra, B. Tyagi, R.V. Jasra, J. Mol. Catal. A: Chem. 223 (2004) 61.
[16] A. Corma, J.M. Serra, A. Chica, Catal. Today 81 (2003) 495.
[17] X. Yang, F.C. Jentoft, R.E. Jentoft, F. Girgsdies, T. Ressler, Catal. Lett. 81 (2002) 25.
[18] Y.Y. Huang, T.J. McCarthy, W.M.H. Sachlter, Appl. Catal. A: Gen. 148 (1996) 135.
[19] Q.H. Xia, K. Hidajat, S. Kawi, Chem. Commun. (2000) 2229, and references therein.
[20] Y.Y. Sun, L. Zhu, H. Lu, R. Wei, S. Lin, D. Jiang, F.S. Xiao, Appl. Catal. A: Gen. 237 (2002) 21.
[21] D.J. Rosenberg, F. Coloma, J.A. Anderson, J. Catal. 210 (2002) 218.
[22] B.M. Reddy, P.M. Sreekanth, Y. Yamada, T. Kobayashi, J. Mol. Catal. A: Chem. 227 (2005) 81.
[23] K. Shibta, T. Kiyoura, J. Kitagawa, T. Sumiyoshi, K. Tanabe, Bull. Chem. Soc. Jpn. 46 (1973) 2985.
[24] K. Arata, S. Akutagawa, K. Tanabe, Bull. Chem. Soc. Jpn. 49 (1973) 390.
[25] R. Sakthivel, H.A. Prescott, J. Deutsch, H. Lieske, E. Kemnitz, Appl. Catal. A: Gen. 20 (2003) 237.
[26] M. Signoretto, S. Melada, F. Pinna, S. Polizzi, G. Cerrato, C. Morterra, Microporous Mesoporous Mater. 81 (2005) 19.
[27] B.M. Reddy, P. Lakshmanan, A. Khan, S. Loridant, C. Lopez-Cartes, T.C. Rojas, A. Fernandez, J. Phys. Chem. 109 (2005) 13545.
[28] S. Pengpanich, V. Meeyoo, T. Rirksomboon, K. Bunyakiat, Appl. Catal. A: Gen. 234 (2002) 221.
[29] B.M. Reddy, P.M. Sreekanth, V.R. Reddy, J. Mol. Catal. A: Chem. 225 (2005) 71.
[30] D.J. Zalewski, S. Alerasool, P.K. Doolin, Catal. Today 53 (1999) 419.
[31] S. Kuba, H. Knözinger, J. Raman Spectrosc. 33 (2002) 325.
[32] B.M. Reddy, P.M. Sreekanth, Y. Yamada, Q. Xu, T. Kobayashi, Appl. Catal. A: Gen. 228 (2002) 269.
[33] J. Gao, Y. Qi, W. Yang, X. Guo, S. Li, X. Li, Mater. Chem. Phys. 82 (2003) 602.
[34] X.M. Lin, L.P. Li, G.S. Li, W.H. Su, Mater. Chem. Phys. 69 (2001) 236.
[35] W.H. Weber, K.C. Hass, J.R. McBride, Phys. Rev. B 48 (1993) 178.
[36] J.R. McBride, K.C. Hass, B.D. Poindexter, W.H. Weber, J. Appl. Phys. 76 (1994) 2435.
[37] C. Morterra, G. Cerratoa, G. Meligrana, M. Signoretto, F. Pinna, G. Strukul, Catal. Lett. 73 (2001) 14.
[38] T. Yamaguchi, K. Tanabe, Mater. Chem. Phys. 16 (1986) 67.
[39] R. Srinivasan, D. Taulbee, B.H. Davis, Catal. Lett. 9 (1991) 1.
[40] C. Morterra, G. Cerrato, M. Signoretto, Catal. Lett. 41 (1996) 101.
[41] D. Spielbauer, G.A.H. Mekhemer, E. Bosch, H. Knözinger, Catal. Lett. 36 (1996) 59.
[42] D. Spielbauer, Dissertation, Universität München, 1995.
[43] A. Corma, V. Fornes, M.I. Juan-Rajadell, J.M. Lopez Nieto, Appl. Catal. 116 (1994) 151.
[44] D. Das, H.K. Mishra, A.K. Dalai, K.M. Parida, Appl. Catal. A: Gen. 243 (2003) 271.
[45] N. Risch, M. Arend, B. Westermann, Angew. Chem. Int. Ed. 37 (1998) 1044.
[46] E.F. Kleinnmann, in: B.M. Trost (Ed.), Comprehensive Organic Synthesis, Vol.2, Pergamon Press, New York, 1991 (Chapter 4.1).
[47] M. Tramontini, L. Angiolini, Mannich Bases: Chemistry and Uses, CRC Press, Boca Raton, FL, 1994.
[48] D.J. Hart, D.C. Ha, Chem. Rev. 89 (1989) 1447.
[49] T. Mukaiyama, K. Kashiwagi, S. Matsui, Chem. Lett. (1989) 1397.
[50] H. Mukaiyama, H. Akamatsu, J.S. Han, Chem. Lett. (1990) 889.
[51] S. Kobayashi, M. Araki, M. Yasuda, Tetrahedron Lett. 36 (1995) 5773.
[52] P.G. Cozzi, B.D. Simone, A. Umani-Ronchi, Tetrahedron Lett. 37 (1996) 1691.
[53] K. Manabe, Y. Mori, S. Kobayashi, Synlett (1999) 1401.
[54] T. Akiyama, J. Takaya, H. Kagoshima, Synlett (1999) 1045.
[55] S. Kobayashi, T. Basujima, S. Nagayama, Synlett (1999) 545.
[56] T.P. Loh, S.B.K.W. Liung, K.L. Tan, L.L. Wei, Tetrahedron 56 (2000) 3227, and references therein.